Biochemical and Biophysical Research Communications 459 (2015) 668–672

Contents lists available at ScienceDirect

Biochemical and Biophysical Research Communications

journal homepage: www.elsevier.com/locate/ybbrc

Solution structure and functional studies of the highly potent equine antimicrobial peptide DEFA1

Matthias Michalek [a], Sascha Jung [a], Mohammad R. Shomali [a], Severine Cauchard [b], Frank D. Sönnichsen [c], Joachim Grötzinger [a, *]

[a] Institute of Biochemistry, Christian-Albrechts-Universität zu Kiel, Olshausenstr. 40, 24098 Kiel, Germany
[b] ANSES, Dozulé Laboratory for Equine Diseases, Bacteriology and Parasitology Unit, 14430 Goustranville, France
[c] Otto Diels Institute of Organic Chemistry, Christian-Albrechts-Universität zu Kiel, Olshausenstr. 40, 24098 Kiel, Germany

ARTICLE INFO

Article history:
Received 13 February 2015
Available online 11 March 2015

Keywords:
Antimicrobial peptides
Horse
Defensins
Structure
NMR spectroscopy

ABSTRACT

Defensins are small effector molecules of the innate immune system that are present in almost all organisms including plants and animals. These peptides possess antimicrobial activity against a broad range of microbes including bacteria, fungi and viruses and act as endogenous antibiotics. α-Defensins are a subfamily of the defensin family and their expression is limited to specific tissues. Equine DEFA1 is an enteric α-defensin exclusively secreted by Paneth cells and shows an activity against a broad spectrum of microbes, including typical pathogens of the horse such as *Rhodococcus equi*, various streptococci strains, *Salmonella choleraesuis*, and *Pasteurella multocida*. Here, we report the three-dimensional structure of DEFA1 solved by NMR-spectroscopy and demonstrate its specific function of aggregating various phospholipids.

1. Introduction

Antimicrobial peptides (AMPs) are small proteins, consisting of ten to fifty amino-acid residues and are ancient weapons against pathogens. AMPs belong to the innate immune system. They are largely abundant in nature (in both animal and plant kingdom) and are typically of cationic nature [1].

Several antimicrobial peptides (AMPs) of equine origin have been identified either at mRNA and/or on protein level in many tissues of the horse [2]. Seven families of antimicrobial peptides were identified, namely lysozymes [3], cathelicidins [4], hepcidins [5], neutrophil antimicrobial peptides [6], NK-lysin [7], psoriasin [8] and defensins [9]. The first equine defensin (DEFB1) was characterized by Davis et al. [10]. Its sequence is similar to the human HBD-2 and showed the typical β-defensin arrangement of disulphide bonds [7]. DEFB1 is expressed in many organs such as lung, spleen, kidney, liver, small intestine and heart [7].

By transcriptional analysis Bruhn et al. [11] showed that an equine small intestine transcript might be a potential equine α-defensin (*DEFA1*) based on its high sequence similarity to Paneth-cell α-defensins (*HD5*) of primates and rodents.

Rhodococcus equi is a severe pathogen of foals and the causal agent of *R. equi* infection, pneumonia or associated diseases. The pathogen is often found together with *Klebsiella pneumoniae* or *Streptococcus zooepidemicus*. Moreover, *R. equi* becomes increasingly pathogenic to humans, in particular to immunocompromised, e. g. HIV infected persons/patients [12,13]. Therefore, the ability of DEFA1 to kill these pathogens was evaluated *in vitro*, revealing a potential as an alternative drug to antibiotherapy against *R. equi* and *S. zooepidemicus* [14]. A recent study provided evidence that DEFA1 could be a promising candidate with reduced cytotoxicity at bacteriolytic concentration *in vitro* [15]. However, assessment of its *in vivo* tolerance remains to be investigated as DEFA1 displays cytotoxicity at higher concentrations.

In a previous study, DEFA1 was expressed in *E. coli* and its antimicrobial activity against different microorganisms was determined [11]. Its mode of action was investigated by studying the membrane-permeabilizing activity using viable bacteria and membrane models. Interestingly, the peptide showed an unusual mode of interaction with liposomes. Whereas most antimicrobial peptides form pores or lesions into the targeted membranes, DEFA1 lead to aggregation of liposomes containing negatively charged lipids.

* Corresponding author. Biochemisches Institut, Christian-Albrechts-Universität zu Kiel, Olshausenstr. 40, 24118 Kiel, Germany. Fax: +49 431 8805007.
E-mail address: jgroetzinger@biochem.uni-kiel.de (J. Grötzinger).

http://dx.doi.org/10.1016/j.bbrc.2015.02.168
0006-291X/

In order to understand the structural traits of this unusual mode of action we solved the three-dimensional structure of this peptide in solution by NMR-spectroscopy and analysed its aggregating function in the presence of lipid vesicles.

2. Materials and methods

2.1. Peptide

The DEFA1 peptide was prepared as described previously [15]. For NMR-spectroscopy the protein was dissolved in 20 mM phosphate buffer pH 5.7. The final concentration was 0.3 mM.

2.2. NMR spectroscopy

NMR measurements were performed on a Bruker Avance 600-MHz spectrometer equipped with a z-gradient triple-resonance cryoprobe. Sequence-specific backbone resonance assignments of DEFA1 were established using two-dimensional DQF-COSY-, TOCSY- (mixing times: 60 ms) and NOESY-spectra (mixing times: 100, 150, 200 and 250 ms). The spectra were acquired at 298 K and referenced to the water resonance at 4.75 ppm. All spectra were processed with NMRPipe [16] and analysed with NMRViewJ [17].

2.3. Structure calculation

Structure calculations were performed using the program CYANA [18]. The structure calculation was based on 230 NOE distance restraints derived from the two-dimensional NOESY experiments. Distances were calibrated using an r^6 function. Three disulphide bonds were defined as 18 distance restraints ranges as follows: $2.0 \leq d(S_i^{\gamma}, S_j^{\gamma}) \leq 2.1$ Å; $3.0 \leq d(C_i^{\beta}, S_j^{\gamma}) \leq 3.1$ Å; $3.0 \leq d(S_i^{\gamma}, C_j^{\beta}) \leq 3.1$ Å. 100 structures were independently calculated and subsequently refined in explicit solvent with the CNS program using the RECOORD protocol and parameters [19]. The ten energetically best structures were selected as the final refined structural ensemble and were deposited (protein data bank accession code: 2mxq). All molecular graphical representations were generated using the programs RIBBONS [20] and GRASP2 [21].

2.4. Fluorescence spectroscopy

Tryptophan-emission fluorescence measurements were performed on a Hitachi F-2500 fluorescence spectrometer (Tokyo, Japan) with an excitation wavelength of 280 nm at 20 °C. 15 μl of LUV lipid suspensions were added from stock solutions of 6.5 mg/ml to a solution of DEFA1 (0.2 μg/ml final concentration) in 50 mM sodium phosphate buffer, pH 5.2 into quartz cuvettes of 1 cm path length (Hellma Analytics, Müllheim, Germany). Emission and excitation bandwidth were set to 10 nm, with the photomultiplier tube voltage of 400 V. Emission spectra were recorded after short incubation from 300 to 400 nm with a scanning speed of 60 nm/min and averaging three scans. Spectra were corrected for baseline and dilution after adding lipid vesicles for each measurement. The data of the tryptophan emission were depicted using Origin 6.0.

2.5. Vesicle preparation

For vesicle preparation lipids composing PE (L-α-phosphatidylethanolamine), PG (L-α-phosphatidyl-DL-glycerol), PS (L-α-phosphatidylserine) or PC (L-α-phosphatidylcholine, Avanti Polar Lipids, Alabaster, USA) were dissolved in chloroform and subsequently evaporated under a nitrogen stream to obtain a thin lipid film. Residual solvent was removed by lyophilisation, followed by rehydration through 2 h shaking in 50 mM sodium phosphate buffer, pH 5.2. The suspension was subjected to three cycles of freezing in liquid nitrogen and thawing in a water bath of 37 °C. Finally, large unilamelar vesicles (LUV) were produced by sonication until the suspension was clear and subsequent size exclusion chromatography using NAP-5 columns (GE-Healthcare, Freiburg, Germany), following the manufacturer's instructions.

2.6. Dynamic light scattering (DLS) measurements

Dynamic light scattering measurements were performed on a Laser-Spectroscatter 201 (RiNA, Berlin, Germany) at an angle of 90° and 20 °C. 10 μl LUV suspensions were diluted twofold and applied to 6 μM DEFA1 in 50 mM sodium phosphate buffer, pH 5.2 mixed carefully and incubated for 3 min at RT. Subsequently, 10 μl were subjected to a quartz cuvette and the size distribution was monitored in 10 subsequent measurements. For data interpretation particles with an occurrence <0.12 were neglected.

2.7. Fluorescence microscopy

The fluorescence microscopic analysis was performed on a CKK41 microscope (Olympus, Hamburg, Germany). The DEFA1 peptide sample (24 μM) was incubated with 1 μl Calcein-loaded LUV suspension composed of PG in 50 mM sodium phosphate buffer, pH 5.2 at RT. Samples were shaken at 1400 rpm for 1 min and incubated for different time periods. After 5 or 30 min, 1 μl of the reaction suspension was transferred onto an object slide, dried in the dark until liquid was evaporated and subsequently analysed under the microscope.

3. Results

3.1. The solution structure of DEFA1

By the use of 2D-TOCSY and NOESY spectra 30 of expected 34 spin-systems were identified. Fig. 1A shows the identified sequential, short and medium contacts. The pattern of these contacts is typical for a β-sheet containing peptide. Fig. 1B shows the number of short, medium and long range contacts identified for each amino-acid residue (Table 1). Most of the long-range contacts are present in the amino- and carboxy-terminal regions suggesting that these two parts build the core of the protein. Fig. 2A shows a representative structure out of the ensemble of the 10 energetically best structures. The structure contains three β-strands (T3–R6; R15–S17; L30–C32) connected by flexible regions as expected for α-defensins. Fig. 2B shows the ensemble of DEFA1 structures. The disulphide linkages were derived in analogy to the reported structures of other α-defensins.

3.2. Comparison with other α-defensins

Sequence analysis of DEFA1 with other α-defensin family members revealed that DEFA1 is the orthologue to human Paneth-cell-specific α-defensin 5 (HD5) [11]. As shown in Fig. 3A–C, the tertiary structure of DEFA1 shows a high similarity to the tertiary structure of human neutrophil peptide 3 (HNP3) and α-defensin 5 (HD5). Like HNP3 and HD5, DEFA1 has a short unstructured N-terminal region, followed by the first β-strand (β1), a first loop connecting β1 to β2 and a second loop connecting β2 and β3. Compared to HD5 and HNP3, the second loop in DEFA1 is more extended. The termini of DEFA1 are further apart from each other compared to the termini of HD5 and HNP3. Fig. 3D–F compares the surface properties of DEFA1, HD5 and HNP3. The distribution of positive charged residues (arginine and lysine) and hydrophobic residues on the surface of DEFA1, HD5 and HNP3 is completely

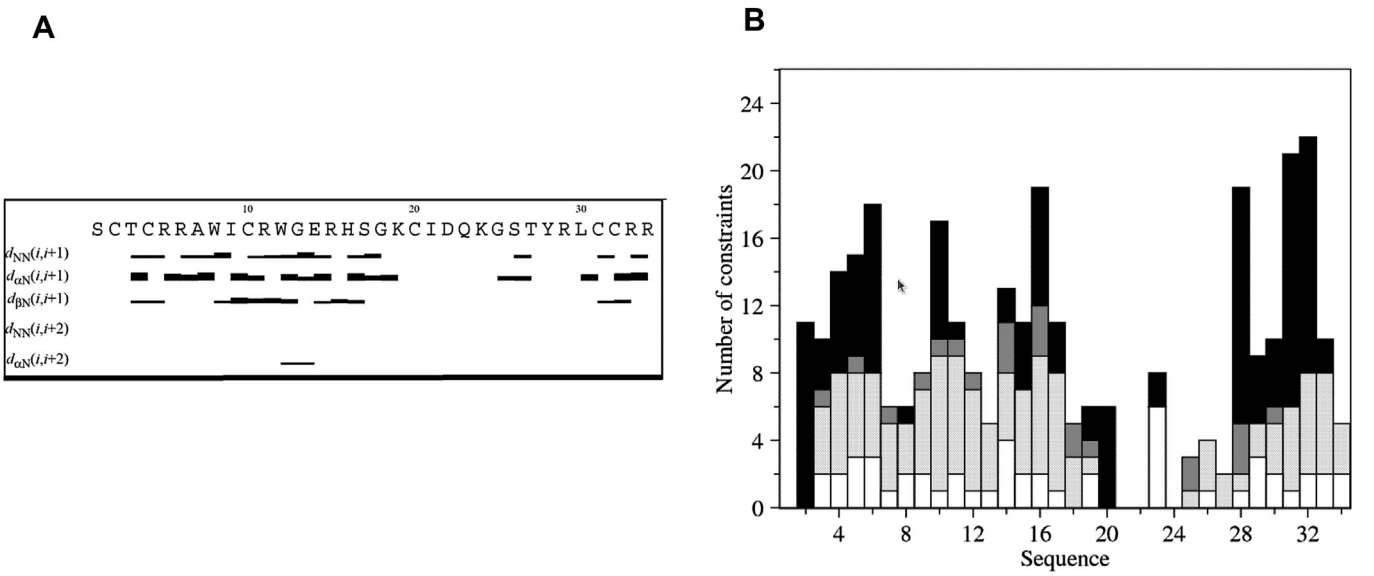

Fig. 1. A) Sequential plot of the identified contacts. Bars represent the correlation between neighbouring protons, e.g. $H^{N}_{(i)}$–$H^{N}_{(i+1)}$. The thickness of the bars corresponds to the intensities of the resonances. B) Sequence distribution of the distance restraints. Bars represent intra-residual- (white), sequential- (light grey), medium range (dark grey) and long range (black) contacts.

different. DEFA1 displays an amphipathic structure with hydrophobic residues forming two hydrophobic areas. Positively charged residues form a hydrophilic belt around the middle of the molecule, separating the two hydrophobic areas. In HD5 and HNP3 this charged belt does not exist and the positive charges are distributed around the whole molecules.

3.3. Lipid interaction of DEFA1

To analyse the lipid interacting properties of DEFA1, tryptophan emission fluorescence spectroscopy was performed. The two tryptophan residues (W8, W12) represent adequate probes for the investigation of lipid interactions, as emission fluorescence spectrum of the indole rings depends on the polarity and refractive index of the environment. In the presence of LUVs composed of PG and PS, the emission spectrum of DEFA1 showed pronounced shifts of 10.5 and 9.5 nm, respectively (Fig. 4A). In contrast, upon addition of PC or PE vesicles, no shifts were observed, indicating the absence of interaction between DEFA1 and zwitterionic phospholipids.

To test whether the interaction of DEFA1 towards lipid vesicles caused aggregation, DLS measurements were performed (Fig. 4B). In the presence of LUVs composed of PG and PS, aggregates with six and four times the size compared with vesicles in the absence of peptide were observed, respectively. Upon longer incubation times, aggregation was even more pronounced, observing with 9 and 7 fold size increase in the vesicle radii. Similar to previous experiments, DEFA1 did not show any lipid interaction nor aggregation of vesicles composed of zwitterionic PC.

To verify vesicle aggregation calcein-loaded LUVs composed of PG were incubated with DEFA1 and analysed under the fluorescence microscope (Fig. 4C). Compared with the vesicle suspension in the presence of the peptide after 5 min incubation, larger aggregates were observed after 30 min.

Table 1
Structural statistics for the best 10 structures of DEFA1. No distance constraint was violated by more than 0.5 Å in any structure. Rmsd = root mean square deviation.

Distance restraints	Number
Intraresidual (|i-j| = 0)	87
Sequential (|i-j| = 1)	64
Medium range (2 ≤ |i-j| ≤ 4)	13
Long range (|i-j| ≥ 5)	48
Disulphide bonds	18
Total	230
Pairwise rmsd	
Mean global backbone rmsd	1.13 ± 0.19 Å
Mean global heavy atom rmsd	1.87 ± 0.23 Å
Pairwise rmsd for secondary structure	
Mean global backbone rmsd	0.63 ± 0.11 Å
Mean global heavy atom rmsd	1.43 ± 0.21 Å
Ramachandran plot (for average structure out of 10 structures)	
Most favoured regions (%)	42.4%
Additional allowed regions (%)	52.4%
Generously allowed regions (%)	4.8%
Disallowed regions (%)	0.3%

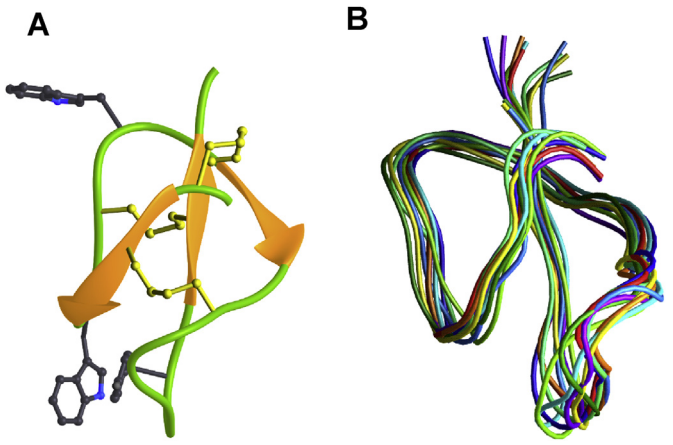

Fig. 2. A) A representative solution structure of DEFA1. Side chains of the disulphide bridges are depicted in yellow and side chains of tryptophan and tyrosine residues in grey. B) Spaghetti representation of the calculated ensemble of DEFA1 structures. (For interpretation of the references to colour in this figure legend, the reader is referred to the web version of this article.)

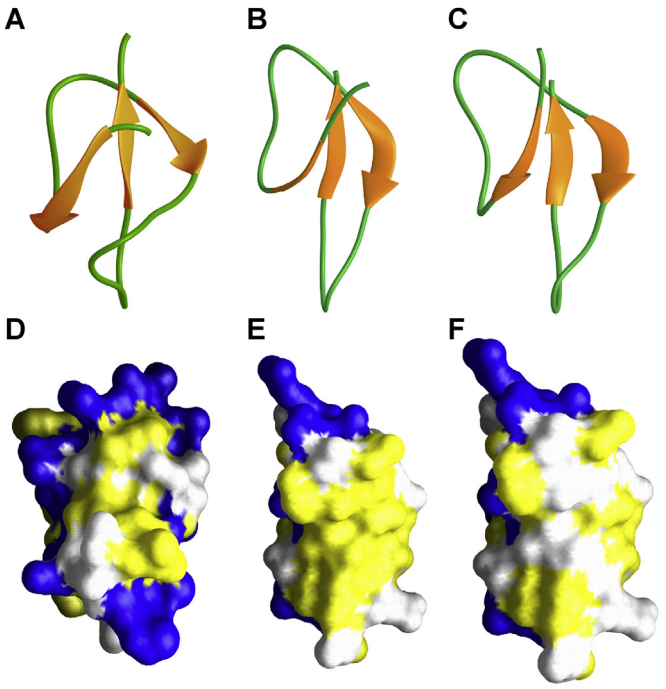

Fig. 3. Comparison of the DEFA1 structure with other α-defensins. Ribbons representations are depicted for A) DEFA1, B) HD5 (Human paneth-cell specific α-defensin, and C) HNP3 (human neutrophil peptide 3). Comparison of the molecular surface properties of D) DEFA1, E) HD5, and F) HNP3. Positive charged residues (Arg and Lys) are coloured blue, whereas hydrophobic areas are coloured yellow.

4. Discussion

Antimicrobial peptides (AMPs) display their bacteria killing functionalities by membrane permeabilization and subsequent breakdown of the membrane potential. By forming stable or transient pores in the membranes' interfacial and hydrophobic regions, the dissipation of essential factors such as ions or small molecules leads to the death of the attacked prokaryotic cell. This function is often described by the barrel-stave or toroidal pore model, respectively [22,23]. Other AMPs disturb the membranes' integrity by concentration-dependent micellisation of certain membrane compartments after binding to the lipid bilayer in a carpet-like manner [24].

Recently, SWTK/R-motifs were identified in the structure of hydramacin-1 (HM1), a host defence peptide of *Hydra magnipapillata*, which facilitate aggregation of phospholipid vesicles and viable bacteria by surficial binding in the membranes' interfacial head-group region [25]. These motifs are located on the surface of the protein and consist of aromatic, cationic and polar amino-acid residues enabling stable binding to phospholipids by electrostatic interaction and hydrogen bonding [25]. These findings led to a new interpretation of the mode of action of such antimicrobial peptides, since aggregation and precipitation of bacteria constitute a function of peptides, described as the barnacle model [26]. Together with the finding that neuromacin, another member of the macin family, aggregates liposomes and bacteria, although containing less pronounced SWTK/R-motifs compared with HM1, the complexity of amino-acid residues that induce aggregation is extended [27]. Similar to HM1, the primary structure of DEFA1 contains tryptophan and tyrosine residues directly flanked by positively charged and polar amino-acid residues. The solution structure of DEFA1 revealed that these aromatic residues (W8, W12, Y28) are located on one half of the peptides' surface and are surrounded by serine (S26), threonine (T27), lysine (K19) and arginines (R5, 6, 11, 29). On the opposite side of DEFA1, amino-acid residues such as histidine (H16), lysines (K19, 24), arginines (R15, 34) and serines (S1, 17) build a conceivable second site for the aforementioned interaction with the head-group regions of biological membranes. This ring-like distribution of amino-acid residues is comparable to what has been shown for the solution structures of HM1 or neuromacin [26,27].

This prompted us to analyse the lipid aggregating property of DEFA1 at pH 5.2, where antimicrobial activity was maximal [11]. DEFA1 showed a lipid binding specificity for anionic phospholipids due to its cationic character, which has been reported for several antimicrobial peptides before [28]. Lipid interaction of DEFA1 was accompanied with aggregation, which was also shown for HM1 and

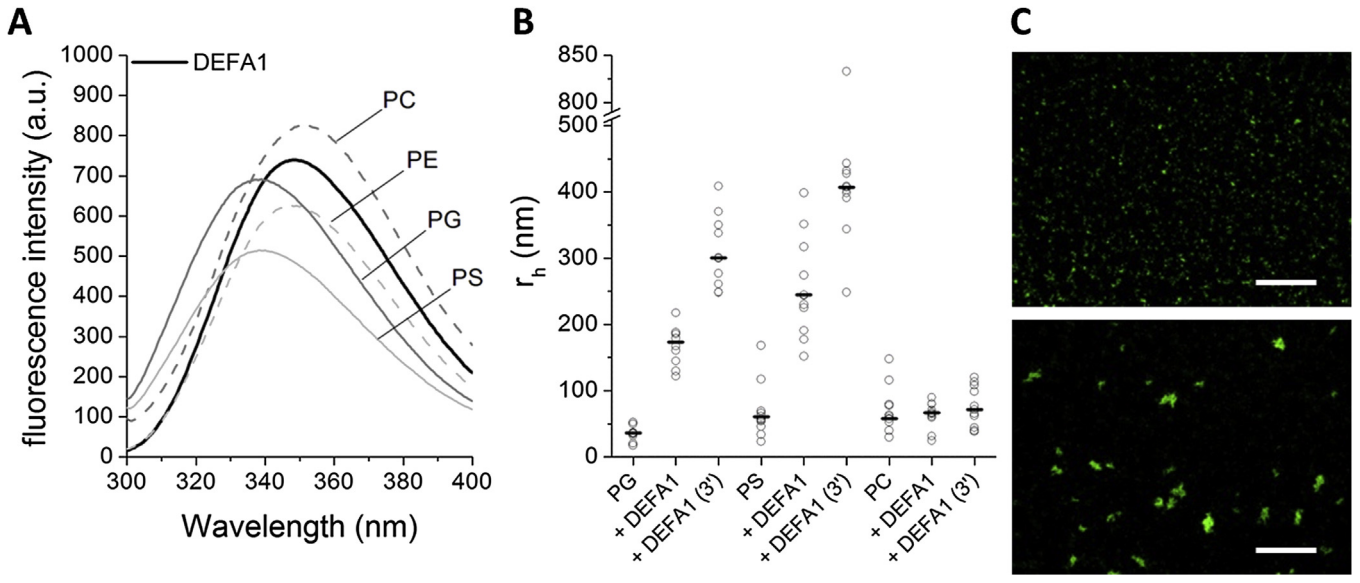

Fig. 4. Lipid interaction of DEFA1 towards phospholipid vesicles. A) Tryptophan emission spectra of 0.2 mg/ml DEFA1 in 50 mM sodium phosphate buffer, pH 5.2 and in the presence of 0.25 mg/ml LUV suspensions composed of various phospholipids. B) DLS measurements of LUV suspensions composed of PG, PS and PC in the absence or in the presence of 6 μM DEFA1 after 3 min of incubation are shown for ten measurements (open circles) and the median (thick bar). Longer incubation periods are depicted (+DEFA1 (3′)). C) Microscopic analysis of Calcein-loaded PG vesicles in the presence of DEFA1 after 5 min (top) and 30 min incubation (bottom). The white bar corresponds to a size of 200 μm.

neuromacin. Since DEFA1 is highly positively charged unlike other α-defensins, absorption of the peptide on the membranes' surface becomes feasible. The ring-like distribution of cationic amino-acid residues facilitates electrostatic interaction with different phospholipid vesicles. This mode of action, termed barnacle model, finally results in extensive peptide-liposome complexes. The data presented here show that membrane interaction is mainly an effect of surface property, i.e. charge and amino-acid distribution, and not a consequence of the common fold of the α-defensin peptide family. This observation was also described for members of the macin or saposin-like protein family [27,29].

The antimicrobial activity of DEFA1 ranges from Gram-negative to Gram-positive bacterial strains and fungi at very low concentrations [11]. Membrane permeabilization was observed against *B. megaterium* and pore formation was postulated to be the key event of cell killing. However, the aggregating activity of DEFA1 in the presence of PG liposomes was shown by CD measurements previously [15] so that the antimicrobial peptide's mode of action appears more complex. It appears feasible that after accumulation on the membranes' surface, DEFA1 induces cell aggregation and finally reaches a threshold concentration, at which membrane permeabilization is achieved and the breakdown of the membrane potential and cell death is accomplished.

Conflict of interest

The authors declare no conflict of interest.

Acknowledgments

This study was supported by the Excellence Cluster 306 'Inflammation at Interfaces' and by grants from the European Regional Development Fund, the Regional Council of Low Normandy, the Institut Francais du Cheval et de l'Equitation and the French Agency for Food, Environmental and Occupational Health Safety.

Transparency document

Transparency document related to this article can be found online at http://dx.doi.org/10.1016/j.bbrc.2015.02.168.

References

[1] R.E. Hancock, R. Lehrer, Cationic peptides: a new source of antibiotics, Trends Biotechnol. 16 (1998) 82–88.
[2] O. Bruhn, J. Grötzinger, I. Cascorbi, S. Jung, Antimicrobial peptides and proteins of the horse–insights into a well-armed organism, Veterinary Res. 42 (2011) 98.
[3] H.A. McKenzie, D.C. Shaw, The amino acid sequence of equine milk lysozyme,, Biochem. Int. 10 (1985) 23–31.
[4] B. Skerlavaj, M. Scocchi, R. Gennaro, A. Risso, M. Zanetti, Structural and functional analysis of horse cathelicidin peptides, Antimicrob. Agents Chemother. 45 (2001) 715–722.
[5] J.P. Oliveira Filho, P.R. Badial, P.H. Cunha, T.F. Cruz, J.P. Araujo Jr., T.J. Divers, N.J. Winand, A.S. Borges, Cloning, sequencing and expression analysis of the equine hepcidin gene by real-time PCR, Veterinary Immunol. Immunopathol. 135 (2010) 34–42.
[6] M.A. Couto, S.S. Harwig, J.S. Cullor, J.P. Hughes, R.I. Lehrer, Identification of eNAP-1, an antimicrobial peptide from equine neutrophils, Infect. Immun. 60 (1992) 3065–3071.
[7] E.G. Davis, Y. Sang, B. Rush, G. Zhang, F. Blecha, Molecular cloning and characterization of equine NK-lysin, Veterinary Immunol. Immunopathol. 105 (2005) 163–169.
[8] T. Leeb, O. Bruhn, U. Philipp, H. Kuiper, P. Regenhard, S. Paul, O. Distl, B.P. Chowdhary, E. Kalm, C. Looft, Assignment of the equine S100A7 gene (psoriasin 1) to chromosome 5p12–>p13 by fluorescence in situ hybridization and radiation hybrid mapping, Cytogenet. Genome Res. 109 (2005) 533.
[9] H. Kuiper, J.L. Williams, O. Distl, C. Drogemuller, Assignment of the PAX6 gene to bovine chromosome 15q25–>q27 by fluorescence in situ hybridization and confirmation by radiation hybrid mapping, Cytogenet. Genome Res. 109 (2005) 533.
[10] E.G. Davis, Y. Sang, F. Blecha, Equine beta-defensin-1: full-length cDNA sequence and tissue expression, Vet. Immunol. Immunopathol. 99 (2004) 127–132.
[11] O. Bruhn, P. Regenhard, M. Michalek, S. Paul, C. Gelhaus, S. Jung, G. Thaller, R. Podschun, M. Leippe, J. Grötzinger, E. Kalm, A novel horse alpha-defensin: gene transcription, recombinant expression and characterization of the structure and function, Biochem. J. 407 (2007) 267–276.
[12] S. Topino, V. Galati, E. Grilli, N. Petrosillo, *Rhodococcus equi* infection in HIV-infected individuals: case reports and review of the literature, AIDS Patient Care STDS 24 (2010) 211–222.
[13] A.V. Yamshchikov, A. Schuetz, G.M. Lyon, *Rhodococcus equi* infection, Lancet Infect. Dis. 10 (2010) 350–359.
[14] O. Bruhn, J. Cauchard, M. Schlusselhuber, C. Gelhaus, R. Podschun, G. Thaller, C. Laugier, M. Leippe, J. Grotzinger, Antimicrobial properties of the equine alpha-defensin DEFA1 against bacterial horse pathogens, Vet. Immunol. Immunopathol. 130 (2009) 102–106.
[15] M. Schlusselhuber, S. Jung, O. Bruhn, D. Goux, M. Leippe, R. Leclercq, C. Laugier, J. Grötzinger, J. Cauchard, In vitro potential of equine DEFA1 and eCATH1 as alternative antimicrobial drugs in rhodococcosis treatment, Antimicrob. Agents Chemother. 56 (2012) 1749–1755.
[16] F. Delaglio, S. Grzesiek, G.W. Vuister, G. Zhu, J. Pfeifer, A. Bax, NMRPipe: a multidimensional spectral processing system based on UNIX pipes, J. Biomol. NMR 6 (1995) 277–293.
[17] B.A. Johnson, R.A. Blevins, NMR View: a computer program for the visualization and analysis of NMR data, J. Biomol. NMR 4 (1994) 603–614.
[18] P. Güntert, Automated NMR structure calculation with CYANA, Methods Mol. Biol. 278 (2004) 353–378.
[19] A.T. Brünger, P.D. Adams, G.M. Clore, W.L. DeLano, P. Gros, R.W. Grosse-Kunstleve, J.S. Jiang, J. Kuszewski, M. Nilges, N.S. Pannu, R.J. Read, L.M. Rice, T. Simonson, G.L. Warren, Crystallography & NMR system: a new software suite for macromolecular structure determination,, Acta Crystallogr. Section D Biol. Crystallogr. 54 (1998) 905–921.
[20] M. Carson, Ribbons 2.0, J. Appl. Crystallogr. 24 (1991) 946–950.
[21] D. Petrey, B. Honig, GRASP2: visualization, surface properties, and electrostatics of macromolecular structures and sequences, Methods Enzym. 374 (2003) 492–509.
[22] G. Baumann, P. Mueller, A molecular model of membrane excitability,, J. Supramol. Struct. 2 (1974) 538–557.
[23] K. Matsuzaki, O. Murase, N. Fujii, K. Miyajima, An antimicrobial peptide, magainin 2, induced rapid flip-flop of phospholipids coupled with pore formation and peptide translocation, Biochemistry 35 (1996) 11361–11368.
[24] Y. Shai, Mechanism of the binding, insertion and destabilization of phospholipid bilayer membranes by alpha-helical antimicrobial and cell nonselective membrane-lytic peptides, Biochim. Biophys. Acta 1462 (1999) 55–70.
[25] M. Michalek, B. Vincent, R. Podschun, J. Grötzinger, B. Bechinger, S. Jung, Hydramacin-1 in action: scrutinizing the barnacle model, Antimicrob. Agents Chemother. 57 (2013) 2955–2966.
[26] S. Jung, A.J. Dingley, R. Augustin, F. Anton-Erxleben, M. Stanisak, C. Gelhaus, T. Gutsmann, M.U. Hammer, R. Podschun, A.M. Bonvin, M. Leippe, T.C. Bosch, J. Grötzinger, Hydramacin-1, structure and antibacterial activity of a protein from the basal metazoan *Hydra*, J. Biol. Chem. 284 (2009) 1896–1905.
[27] S. Jung, F.D. Sönnichsen, C.W. Hung, A. Tholey, C. Boidin-Wichlacz, W. Haeusgen, C. Gelhaus, C. Desel, R. Podschun, V. Waetzig, A. Tasiemski, M. Leippe, J. Grötzinger, Macin family of antimicrobial proteins combines antimicrobial and nerve repair activities, J. Biol. Chem. 287 (2012) 14246–14258.
[28] G. Zou, E. de Leeuw, C. Li, M. Pazgier, P. Zeng, W.Y. Lu, J. Lubkowski, W. Lu, Toward understanding the cationicity of defensins. Arg and Lys versus their noncoded analogs, J. Biol. Chem. 282 (2007) 19653–19665.
[29] B. Olmeda, B. Garcia-Alvarez, J. Perez-Gil, Structure-function correlations of pulmonary surfactant protein SP-B and the saposin-like family of proteins, Eur. Biophys. J. 42 (2013) 209–222.